

Star-Forming Compact Groups (SFCGs): An ultraviolet search for a local sample

Jonathan D. Hernández-Fernández¹, C. Mendes de Oliveira¹

ABSTRACT

We present a local sample ($z < 0.15$) of 280 Star-Forming Compact Groups (SFCGs) of galaxies identified in the ultraviolet Galaxy Evolution EXplorer (GALEX) All-sky Imaging Survey (AIS). So far, just one prototypical example of SFCG, the Blue Infalling Group, has been studied in detail in the Local Universe. The sample of SFCGs is mainly the result of applying a Friends-of-Friends group finder in the space of celestial coordinates with a maximum linking-length of 1.5 arcmin and choosing groups with a minimum number of four members of bright UV-emitting $17 < FUV < 20.5$ sources (mostly galaxies) from the GALEX/AIS catalogue. The result from the search are 280 galaxy groups composed by 226, 39, 11 and 4 groups of four, five, six and seven bright ultraviolet (UV) members, respectively. Only 59 of these 280 newly identified SFCGs have a previous catalogued group counterpart. Group redshifts are available for at least one member in 75% of the SFCGs, and over 40% of the SFCGs have redshifts measured for two or more galaxies. Twenty-six of the SFCGs appear to be located in the infalling regions of clusters with known redshift. The SFCG sample presents a combination of properties different from the group samples studied up to now, such as low velocity dispersions ($\sigma_{1-\sigma-s} \sim 120 \text{ km s}^{-1}$), small crossing-times ($H_0 t_c \sim 0.05$) and high star-formation content (95% of star-forming galaxies). This points to the SFCGs being in an evolutionary stage distinct from those groups selected in the optical and near-infrared ranges. Once redshifts are obtained to discard interlopers, SFCGs will constitute a unique sample of star forming compact groups.

Subject headings: galaxies: clusters: general, galaxies: evolution, galaxies: star formation, ultraviolet: galaxies

1. Introduction

Over the last few years, the *preprocessing scenario* has been identified as a significant mode of star-formation quenching and morphological transformation in the context of environmental galaxy evolution (Fujita 2004; Moss 2006; Cortese et al. 2006; Wilman et al. 2009; Just et al. 2010; Wetzel et al. 2013; Hou et al. 2014). In this scenario, environmental processes drive the evolution of galaxies within groups before they fall into a massive cluster. In support of this scenario, McGee et al. (2009) found that simulated clus-

ters up to $z=1.5$ have had a significant fraction of their galaxies accreted through galaxy groups. For instance, $10^{14.5} h^{-1} M_\odot$ mass clusters at $z=0$ have had ~ 40 per cent of their galaxies with stellar masses $M_\star > 10^9 h^{-1} M_\odot$ accreted through haloes with masses greater than $10^{13} h^{-1} M_\odot$. At higher redshifts, fewer galaxies are accreted through massive haloes. Only ~ 25 per cent of galaxies have been accreted through $10^{13} M_\odot$ groups into $10^{14.5} h^{-1} M_\odot$ clusters at $z=1.5$.

The unique case in the local Universe considered as an ongoing example of the preprocessing scenario is the *Blue Infalling Group* (BIG); the region with the highest density of star forming systems ever observed in the Local Universe (Cortese et al. 2006). Only this case of an infalling group with bursts of star formation induced

¹Departamento de Astronomia, Instituto de Astronomia, Geofísica e Ciências Atmosféricas da Universidade de São Paulo, Rua do Matão 1226, Cidade Universitária, 05508-090, São Paulo, Brazil; jonatan.fernandez@iag.usp.br

by ram-pressure has been observed in $H\alpha$ in the Local Universe and the group shows a wealth of structures hosting current star formation activity such as tidal streams or clustered knots, as it can be seen in figure 1. Similar examples of star-forming infalling groups in the Local Universe are expected to be rare since the current merger rate in clusters is considerably lower than in the past (e.g. Gottlöber et al. 2001). In figure 1 we show the comparison between the $H\alpha$ net-flux (left panel) and the Galaxy Evolution EXplorer (GALEX) NUV image (right panel) of the BIG. As it can be easily seen in this figure, even in the cases where there are just faint clustered knots of $H\alpha$ emission in the optical image, bright ultraviolet (UV) counterparts can be found in the GALEX image. Consequently, GALEX catalogues provide an excellent chance to find analogues of BIG.

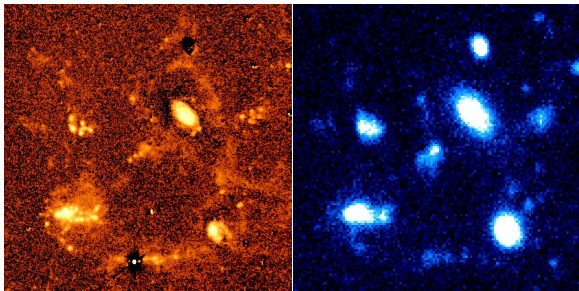


Fig. 1.— **Two views of the Blue Infalling Group (BIG). Left panel: $H\alpha$ net-flux image of the BIG taken from GOLD Mine database (<http://goldmine.mib.infn.it>). Right panel: GALEX NUV image of the BIG. The size of the image is 3.25×3.25 arcmin², corresponding to 108 kpc.**

The *double-cycle scenario* recently proposed by Dressler et al. (2013) presents some tension with the view of BIG as an ongoing event of group preprocessing. The authors, studying a sample of intermediate redshift clusters, point that poststarburst spectra trace accretions in passive galaxies, while a starburst spectra signal minor mergers in star-forming galaxies. In this picture, spectroscopically identified post-starbursts constitute a minority of all recently terminated starbursts, largely ruling out the typical starburst as a quenching event in all but the densest environments. A sample of Star-Forming Compact Groups (SFCGs) analogues of the BIG, can be

an excellent chance to assess the relative predominance of starbursts and post-starbursts in the process of star-formation quenching and morphological transformation within infalling groups.

Differently from galaxies in clusters, *galaxies in groups* represent a large contribution of the giant galaxy population in the nearby universe (Cox 2000; Eke et al. 2005). More specifically, for a local volume-limited sample of luminous $M_r < -18$ galaxies from Nurmi et al. (2013), 40% of galaxies are considered isolated, 16% are galaxies in pairs, 35% of the galaxy population is in groups of $3 \leq n_{\text{gal}} < 30$ members and just 9% belong to galaxy clusters of 30 members or more. Nurmi et al. (2013) apply a Friends-of-Friends (FoF) algorithm with a variable linking-length depending on redshift and calibrated with a local sample of real galaxy groups. Further, detailed studies of galaxy interactions and environmental processes in their most frequent environment in the very moment when they occur are indispensable to adequately describe galaxy evolution. In this respect, $H\alpha$ imaging allows us to identify where within the group galaxies they are forming stars normally and where they have had their star formation enhanced or depressed by interactions with the other group members and other environmental processes i.e. gas stripping, starvation (Koopmann & Kenney 2004). Interestingly, SFCGs are ideal targets where $H\alpha$ emission maps are more easily obtained, particularly for those instruments with relatively small fields of view (e.g. BTFi, Mendes de Oliveira et al. 2013).

As an additional product of strong *galaxy interactions*, stellar material may be ejected in the surroundings. In the situation when this material is dynamically bound, it may be the progenitor of a population of the so-called tidal dwarf galaxies (Duc et al. 2000; Iglesias-Páramo & Vílchez 2001) and/or HII extragalactic clumps (Mendes de Oliveira et al. 2004; Boquien et al. 2010; Urrutia-Viscarra et al. 2014). Otherwise, it would contribute to the intra-group(-cluster) light. In this respect, Domainko et al. (2006) show that ram-pressure stripping can account for $\sim 10\%$ of the overall observed level of metal enrichment in the intracluster medium (ICM) within the virial region. A detailed analysis of the frequency and properties of the population of dwarf galaxies, HII extragalactic regions and intragroup light

in the sample of SFCGs would provide insights about the contribution of galaxy interactions to group/cluster components.

It is broadly understood that galaxy groups go through an *evolutionary sequence* starting in poor groups as the Local Group and evolving towards those galaxy groups dominated by a very massive elliptical galaxy called fossil groups (after Ponman et al. 1994), or less massive versions of them (Jones et al. 2003; D’Onghia et al. 2005; Zabludoff 2007; Grebel 2007; Gallagher et al. 2010), or yet massive elliptical galaxies in the field (Mamon 1986; Williams & Rood 1987). In this scenario, *compact groups* represent the evolutionary link between these apparently unrelated extragalactic objects.

Such as it can be seen in literature, a detailed study of a sample of compact groups of star-forming galaxies can shed light in a broad ensemble of aspects of galaxy evolution in groups. Section 2 describes the selection of a sample of this type, starting from catalogues of pure UV sources and also presents the final sample including observational information and basic properties. In Section 3, several aspects of the SFCG sample are analyzed and compared with three other prototypical compact group samples: the optically-selected Hickson Compact Group (HCG, Hickson 1982; Hickson et al. 1992) sample, the near-infrared-selected and velocity-filtered 2MASS Compact Group (2MCG, Díaz-Giménez et al. 2012) sample and the catalogue A of compact groups selected in the Sloan Digital Sky Survey by McConnachie et al. (SCGA, 2009). Section 4 places the SFCG sample in the context of the Local Universe providing additional information about their galaxy members, cluster and group counterparts and also, the close surroundings of its groups.

2. Selection of the SFCG sample

Our approach is focused on searching for compact groups composed or dominated by star-forming galaxies in the Local Universe.

2.1. An all-sky sample of bright ultraviolet-emitting sources

We choose the All-sky Imaging Survey (AIS) from GALEX as the most suitable database to extract large samples of star-forming galaxies in the

Local Universe. The GALEX/AIS is the largest effective sky area, more than 22000 square degrees, observed in UV in a homogeneous way down to a typical depth of $FUV \sim 20$ AB mag and $NUV \sim 21$ AB mag (Bianchi et al. 2014).

We select those UV sources with an apparent FUV magnitude of $17 < FUV < 20.5$, because the FUV band is tracing the emission of stars with shorter lifetimes in comparison with the NUV (Martin et al. 2005; Haines et al. 2008). We note that the UV-bright galaxies in BIG are approximately in this magnitude range. This small magnitude interval is chosen to increase the probability of selecting galaxies that are physically associated with each other (by not being at greatly differing distances), and with a young stellar component which is similar so that all group members would be significant participants in the total star formation of the group. Given that the redshift distribution of GALEX sources is mostly restricted to $z \lesssim 0.2$ (Wyder et al. 2005), this further biases the selection towards galaxies with a high level of star formation activity in the Local Universe.

We stress that the selection using the GALEX FUV band allows us to also include in our sample the low-mass star-forming galaxies, without a bright counterpart in the optical bands, and therefore, which rarely included in searches of groups performed in the optical and near-infrared (i.e. Hickson 1982; Hickson et al. 1992; McConnachie et al. 2009; Díaz-Giménez et al. 2012). The searches of galaxy groups extracted from optical and near-infrared surveys favour galaxy groups constituted by the massive examples of the galaxy population i.e. a *stellar-mass biased search*, while a search of groups of UV-bright galaxies finds those galaxies which encompass the bulk of the current star formation of the galaxy population, i.e. a *star-formation biased search*. A test of an ultraviolet search over the galaxy members of the HCG catalogue is included in Subsection 3.3 and confirms this statement. In spite of that, one has to keep in mind that the SFCGs can indeed contain passive galaxies as close companions of those star-forming galaxies with a high UV emission.

In addition, the following UV colour constraint $-1.50 \leq (FUV - NUV)_d \leq 2.75$ is included in the source selection. $(FUV - NUV)_d$ corresponds to the GALEX UV colour corrected from Galactic extinction, following the Cardelli extinction law

(Cardelli et al. 1989) and a value of the ratio of total to selective absorption in the V band of $R_V=3.1$. This has been shown to be very useful in rejecting ‘blue artifacts’, commonly found throughout GALEX fields, particularly in the neighbourhood of saturated stars and also over galactic regions with a diffuse UV emission, which do not correspond to real sources. Indeed, this constraint could reject some real UV galaxies but we prefer to include this condition for the sake of purity of the input UV sample and the efficiency of the search.

Furthermore, we take advantage of the GALEX flag `nuv_artifact` which is a photometric-quality estimator. `nuv_artifact` consists in a bitwise-encoded unsigned integer, each of which is the bitwise logical ‘OR’ of some or none of a set of nine possible situations (see <http://galex.stsci.edu/GR6/?page=ddfaq#6> for a detailed description of each situation). Criteria about the source brightness for flagging one source are generous, meaning that false-positives are common, especially for ‘edge’ flags i.e. `nuv_artifact=1`. `nuv_artifact` increases its value as a larger number of situations affects the UV source. We therefore consider that selecting sources with `nuv_artifact≤1` is sufficient for a complete and sufficiently reliable source extraction.

Given that we search for compact groups from a sample without information about the nature of the UV sources, we do not know a priori whether the UV source will be a star or a galaxy. Because of that, we try to minimize the effects of contamination by stars by restricting our search to sources beyond 15 degrees of the Galactic Plane i.e. $|b|≥15$ deg.

We download a set of photometric parameters for a sample with the previous constraints running the following SQL code in the CASJobs service of GALEX webpage (<http://galex.stsci.edu/casjobs>):

```
SELECT p.ra, p.dec, p.fuv_mag, p.nuv_mag,
p.e_bv, p.glon, p.glat, q.photoExtractID,
p.objid, q.mpstype
FROM PHOTOOBJALL as p, PHOTOEXTRACT as q
WHERE (p.fuv_mag BETWEEN 17.0 and 20.5)
AND (((fuv_mag-(E_bv*8.376))
      -(nuv_mag-(E_bv*8.741)))
      BETWEEN -1.50 AND +2.75 )
AND ((p.glat<-15.0) OR (p.glat>+15.0))
AND (p.nuv_artifact<=1)
```

```
AND (q.mpstype='AIS')
AND (p.photoExtractID=q.photoExtractID)
```

The result from this SQL query is a catalogue containing 925428 sources.

Due to the GALEX survey strategy, sky regions at the outermost parts of the fields and the UV sources in these regions are systematically observed by neighboring fields i.e. there is significant overlapping. We identify duplicate objects by cross-matching the GALEX sample with itself, using a 6 arcsec search radius, slightly larger than 4.2 and 5.3 arcsec angular resolution of the GALEX FUV and NUV images, respectively (Morrissey et al. 2007).

2.2. Grouping UV sources with the Friends-of-Friends Algorithm

The search for compact groups is done applying a Friends-of-Friends (FoF) algorithm to the previous sample of bright UV sources in the space of celestial coordinates imposing a maximum linking-length. This approach was originally applied by Turner & Gott (1976) to a sample of galaxies from the *Catalogue of galaxies and of clusters of galaxies* of Zwicky et al. (1961, 1968). The upper limit of the linking-length is set to 1.5 arcmin, which corresponds to a projected distance of ~ 88 kpc at $z=0.05$ in the cosmological model used in this work and characterized by $H_0=70$ km s $^{-1}$ Mpc $^{-1}$, $\Omega_m=0.3$ and $\Omega_\Lambda=0.7$. This criterion is included to accept only those groups that are sufficiently compact and also, easily observable with relatively small field instrumentation (e.g. Mendes de Oliveira et al. 2013). The IDL code of the FoF algorithm¹ (Blanton 2001) selects a set of groups whose elements are linked by sky distances less or equal to the linking-length, labeling each group by their number of elements. This code belongs to the IDLUTILS library from the Princeton/MIT Sloan Spectroscopy Home Page (http://spectro.princeton.edu/idlutils_doc.html). The output group catalogue contains 1447 compact groups of UV bright sources including both galaxy and stellar objects. We have found that about 960 of these groups surround the Large and the Small Magellanic Clouds and the bulk of them are projected groups of open star clusters or parts of these two galaxies.

¹http://spectro.princeton.edu/idlutils_doc.html#SPHEREGROUP

2.3. Cross-matching with galaxy catalogues

Knowing that the search of groups of UV sources is done without *a priori* information about the object type and the redshift of the UV source, we crossmatch the output sample of groups of UV sources with the galaxy catalogues compiled by NASA/IPAC Extragalactic Database (NED) applying a matching radius of 6 arcsec in order to retrieve the object type and redshift of each UV source. The cross-matching is provided by NED through the service “Build Data Table from Input List” in its option “Near Name/Position Cross-Matching”: (<http://ned.ipac.caltech.edu/forms/nnd.html>). In the few cases that NED provides more than one counterpart inside the matching circle, we choose an unique source following this hierarchy in priority (1) the galaxy with redshift counterpart (2) the source classified as “galaxy” (3) the nearest source.

2.4. Selection of galaxy group candidates and SFCG catalogue

We only include in the final catalogue of SFCGs those groups with four or more UV sources ($n_{UV} \geq 4$) which respect at least one of the two following criteria:

- groups with at least three UV sources compiled as “galaxy” by NED $n_{gal} \geq 3$ (i.e. three galaxies) or,
- groups with at least two galaxies with redshift counterpart within a redshift interval of $\Delta z / (1+z) = 0.004$ (i.e. two accordant redshifts)

Visually checking the close neighborhood of the groups of UV-emitting sources in GALEX and optical images, we know that these groups can include galaxies without UV emission (i.e. red galaxies) and/or UV galaxies that are so optically faint that they are missed by NED. Knowing this fact, we want to be generous in these first constraints, given that the actual number of galaxy members in each group should be greater than its number of UV sources (n_{UV}) or the number of UV sources compiled as galaxies by NED (n_{gal}).

The previous constraints give an output of 280 compact groups of UV-emitting galaxies with the following multiplicity distribution $N(n)$: 226, 39, 11 and 4 groups with four, five, six and seven UV members, respectively. This multiplicity distribution follows very accurately a power law as $N(n) \sim n^{-\alpha}$ with $\alpha_{UV} = 7.54 \pm 0.49$. As a reference the HCGs follows a multiplicity distribution also well fitted by a power law with $\alpha_{HCG} = 5.25 \pm 0.62$. Therefore, the multiplicity distribution of the SFCG sample is steeper than the multiplicity distribution of the HCG sample. The latter sample is, in addition, poor in UV-bright star-forming galaxies as it is shown in Subsection 3.3. This fact is in general agreement with the weaker clustering of blue galaxies in comparison with red galaxies (e.g. Zehavi et al. 2011).

Celestial coordinates, group redshift (z_{UV}) when available and information in other group properties are shown in Table 1, where SFCGs are ordered by increasing UV richness n_{UV} and increasing right ascension. Table 2 compiles celestial coordinates, NED redshifts when available and GALEX magnitudes for the group UV-bright galaxy members ordered by increasing group ID and increasing right ascension. The values for z_{UV} correspond to the median redshift of the n_z UV galaxies with known redshift. In Table 1, m_z is the number of galaxies with known redshifts within a velocity interval of $|\Delta v_{l-o-s}| \leq 10^3 \text{ km s}^{-1}$, where Δv_{l-o-s} is the l-o-s velocity difference with respect to the group redshift i.e.:

$$\Delta v_{l-o-s} = c \left(\frac{z_{memb} - z_{UV}}{1 + z_{UV}} \right). \quad (1)$$

If there is no known redshift associated to the UV galaxies of a specific SFCG, i.e. $n_z = 0$, we label the redshift value with zero in Table 1, $z_{UV} \equiv 0$. This approach yields 212 group redshifts ($\approx 76\%$) of the whole sample), among which 97 SFCGs with $m_z = 1$ ($\approx 35\%$), 74 SFCGs with $m_z = 2$ ($\approx 26\%$), 36 SFCGs with $m_z = 3$ ($\approx 13\%$) and 5 SFCGs with $m_z = 4$ ($\approx 2\%$). There are no SFCGs with more than $m_z = 4$. In addition, we provide the angular radius r_θ of each SFCG, computed as the square-root of the quadratic average of angular distances r_i of galaxy members to the group center i.e.:

$$r_\theta^2 = \left(\sum r_i^2 \right) / (n_{UV} - 1). \quad (2)$$

We also provide a collection of stamps for the whole SFCG sample in the optical and ultraviolet spectral ranges. The optical images come from the R band of the POSS2/UKSTU surveys and the ultraviolet images correspond to the NUV band from GALEX. The images are fully public and added as additional on-line only material in Figure A1 of Appendix.

Table 1: SFCG catalogue

ID	RA _g [h:m:s]	Dec _g [d:m:s]	z _{UV}	n _{UV}	n _{gal}	n _z	m _z	r _θ [arcmin]	R _{ij} [kpc]	σ _{l-o-s} [km s ⁻¹]
(1)	(2)	(3)	(4)	(5)	(6)	(7)	(8)	(9)	(10)	(11)
1	0:00:23	-22:35:14	0	4	4	0	0	0.913	-1	-1
2	0:01:23	13:06:32	0.017899	4	4	3	3	1.611	32.94	193.85
3	0:11:22	-53:57:20	0.041719	4	3	1	1	1.249	-1	-1
4	0:13:19	-41:34:47	0	4	3	0	0	1.027	-1	-1
5	0:14:09	-22:33:51	0	4	4	0	0	1.149	-1	-1
6	0:17:46	-69:08:55	0	4	3	0	0	1.336	-1	-1
7	0:18:29	-42:07:39	0.093258	4	3	1	1	0.891	-1	-1
8	0:18:39	-35:57:01	0.012953	4	4	2	2	0.888	-1	-1
9	0:21:29	38:05:07	0.035708	4	3	2	2	1.161	-1	-1
10	0:22:41	-20:34:38	0.051799	4	3	1	1	1.041	-1	-1
11	0:31:14	-25:29:44	0.092950	4	4	2	2	1.091	-1	-1
12	0:34:30	39:35:15	0.019458	4	2	2	2	1.634	-1	-1
13	0:37:08	-63:26:26	0.041095	4	3	1	1	0.984	-1	-1
14	0:37:42	-9:03:24	0.076528	4	4	3	3	0.761	74.83	228.04
15	0:37:56	-25:04:18	0.063567	4	3	3	2	1.152	-1	-1
16	0:48:02	-63:09:10	0.086353	4	4	2	1	1.087	-1	-1
17	0:48:58	-45:46:13	0	4	4	0	0	0.809	-1	-1
18	0:49:11	-18:17:43	0.159397	4	3	1	1	1.461	-1	-1
19	0:51:27	-23:12:56	0	4	3	0	0	0.658	-1	-1
20	0:52:11	-1:07:02	0.041300	4	4	3	2	0.596	-1	-1
...
261	17:49:58	68:24:19	0.051225	5	4	3	3	1.190	53.04	219.04
262	21:27:56	-46:38:34	0.046689	5	5	1	1	0.979	-1	-1
263	21:35:23	-49:56:05	0.054924	5	3	2	2	0.870	-1	-1
264	23:16:44	-41:39:20	0	5	4	0	0	1.304	-1	-1
265	23:56:08	-17:14:21	0	5	5	0	0	0.990	-1	-1
266	0:25:12	-60:37:48	0.031292	6	6	1	1	1.141	-1	-1
267	1:39:14	-74:25:23	0	6	3	0	0	1.023	-1	-1
268	2:34:18	-73:43:12	0	6	3	0	0	1.339	-1	-1
269	3:21:01	-33:54:17	0.070421	6	5	4	3	1.144	179.78	224.71
270	4:06:11	-36:55:48	0	6	4	0	0	0.995	-1	-1
271	4:49:33	-73:04:09	0.027543	6	3	2	2	1.263	-1	-1
272	8:20:05	21:04:17	0.017462	6	4	3	1	1.583	-1	-1
273	11:14:32	0:51:08	0.069070	6	6	5	4	1.519	106.41	57.16
274	12:21:14	49:27:34	0.045355	6	5	4	2	1.354	-1	-1
275	15:21:59	3:33:36	0.084655	6	5	4	4	0.701	72.12	268.79
276	21:55:29	-20:51:46	0.066913	6	5	1	1	1.335	-1	-1
277	2:05:03	-74:51:50	0	7	3	0	0	1.597	-1	-1
278	7:41:56	16:49:33	0	7	4	0	0	1.103	-1	-1
279	13:07:17	13:38:57	0.063226	7	6	5	1	1.704	-1	-1
280	23:16:45	9:48:57	0	7	3	0	0	1.114	-1	-1

(1) ID number of the SFCG ordered by increasing UV richness (column 5) and increasing right ascension (column 2), (2) and (3) R.A. [h:m:s] and Dec. [d:m:s] of group center, (4) group redshift, (5) number of UV members, (6) n_{UV} compiled as ‘galaxy’ by NED, (7) n_{UV} with a redshift counterpart, (8) n_{UV} with a known l-o-s velocity within 2000 km s⁻¹ centered at the group redshift, (9) group angular radius in arcmin, (10) median inter-galaxy physical separation in kpc and (11) l-o-s velocity dispersion derived by the gapper method (Beers et al. 1990). For $m_z=3$, the relative uncertainty in σ_{l-o-s} corresponds to 50% and for $m_z=4$ corresponds to 41% following $(\sigma/\delta\sigma)=\sqrt{2(m_z-1)}$ (e.g. Proctor et al. 2011).

Table 2: SFCG galaxy catalogue

ID	ID _{memb}	RA _{memb} [deg]	Dec _{memb} [deg]	z_{memb}	g_{memb}	FUV _{memb} [AB mag]	NUV _{memb} [AB mag]
(1)	(2)	(3)	(4)	(5)	(6)	(7)	(8)
1	1	0:00:18.98	-22:34:33.2	0	0	20.2714	19.9779
1	2	0:00:21.87	-22:35:16.4	0	0	20.2043	19.9377
1	3	0:00:24.05	-22:35:19.7	0	0	19.3392	19.2220
1	4	0:00:26.82	-22:35:44.9	0	0	20.0727	19.8536
2	1	0:01:15.17	13:06:48.3	0.018646	1	18.5922	18.1860
2	2	0:01:20.07	13:06:40.3	0.017899	1	16.7561	16.2019
2	3	0:01:26.22	13:06:45.1	0.017532	1	17.1312	16.6332
2	4	0:01:29.52	13:05:54.9	0	0	19.2810	19.2182
3	1	0:11:20.38	-53:57:21.6	0	-1	20.2101	20.5555
3	2	0:11:21.11	-53:58:51.2	0	0	20.0492	19.6655
3	3	0:11:22.08	-53:57:13.3	0	0	19.9107	19.7047
3	4	0:11:24.55	-53:55:52.3	0.041719	0	17.7296	17.3873
4	1	0:13:15.43	-41:34:16.3	0	0	20.2139	19.7874
4	2	0:13:16.15	-41:35:44.2	0	0	20.2478	19.4746
4	3	0:13:18.35	-41:34:23.5	0	-1	18.2981	18.3077
4	4	0:13:24.64	-41:34:42.6	0	0	19.8293	19.2635
5	1	0:14:04.24	-22:33:09.7	0	0	20.2563	20.0467
5	2	0:14:07.62	-22:33:47.2	0	0	19.9924	19.2451
5	3	0:14:09.35	-22:34:04.8	0	0	20.1528	19.8885
5	4	0:14:14.88	-22:34:22.1	0	0	19.9073	19.6148
...
278	2	7:41:53.17	16:49:43.9	0	0	19.1374	18.9651
278	3	7:41:53.85	16:49:57.6	0	0	19.9631	19.5871
278	4	7:41:55.01	16:49:55.1	0	-1	20.0733	19.3963
278	5	7:41:57.17	16:49:30.1	0	0	19.8613	21.1990
278	6	7:41:59.39	16:49:31.6	0	0	18.7801	18.2003
278	7	7:42:02.43	16:48:30.7	0	-1	17.3001	17.6996
279	1	13:07:10.80	13:40:50.6	0	-1	19.9962	19.8683
279	2	13:07:11.70	13:39:33.1	0.027162	0	18.7777	18.2494
279	3	13:07:12.74	13:38:48.5	0.100102	0	20.2559	19.7801
279	4	13:07:17.56	13:38:47.7	0.026784	0	18.6093	18.0461
279	5	13:07:19.04	13:38:24.2	0	0	17.8783	17.3566
279	6	13:07:21.07	13:37:43.7	0.099919	0	20.0560	19.1825
279	7	13:07:26.39	13:38:29.6	0.063226	1	19.2524	18.8211
280	1	23:16:42.17	9:50:15.5	0	-1	19.6095	19.3379
280	2	23:16:42.63	9:47:32.3	0	0	18.3754	17.8370
280	3	23:16:43.20	9:48:58.2	0	-1	19.2525	18.8421
280	4	23:16:43.27	9:49:44.8	0	-1	19.2900	18.8361
280	5	23:16:47.03	9:48:45.5	0	-1	19.3780	19.0168
280	6	23:16:47.67	9:48:17.6	0	0	18.2314	17.5936
280	7	23:16:48.49	9:49:02.0	0	0	19.2150	18.9493

(1) ID number of the SFCG, (2) ID number of the SFCG galaxy ordered by increasing right ascension (column 3), (3) and (4) R.A. [h:m:s] and Dec. [d:m:s] of UV-bright galaxy member, (5) galaxy redshift, (6) group membership code (1: velocity-accordant galaxy member, 0: non-member galaxy or unknown redshift, -1: non-NED galaxy), (7) and (8) FUV and NUV (AB) magnitudes corrected for Galactic extinction.

3. Characterization of the SFCG sample and comparison with other groups samples

3.1. Redshift and physical size distribution and the comparison with other group samples

Figure 2 shows the redshift and physical diameter distribution of the subsets of SFCGs, the HCGs and the SCGAs with $m_z \geq 3$ i.e. three or more galaxy members within a l-o-s velocity $|\Delta v_{l-o-s}| \leq 10^3 \text{ km s}^{-1}$ centered at the group redshift. The 2MCG sample has $m_z \geq 4$ by construction. Figure 2 also shows the SFCG subsets with $m_z=1$ (horizontal cyan ellipses) and those SFCGs with $m_z=2$ (vertical violet ellipses). The HCG sample studied here consists of 91 groups where the HCG54 is not included in the graph because this system has been considered to be a single galaxy rather than a group (Verdes-Montenegro et al. 2002; Torres-Flores et al. 2010). With respect to the SCGA, instead of choosing the catalogue B ($r' < 21$), we chose catalogue A ($r' < 18$), because this magnitude cut of catalogue A is comparable to the completeness limit of the GALEX/AIS (Martin et al. 2005).

The physical diameter $2r_{\text{phy}}$ is defined here as the double of the physical radius $r_{\text{phy}} = r_\theta \times d_\theta(z_{UV})$ with $d_\theta(z_{UV})$ the angular-diameter distance (e.g. Carroll et al. 1992). The angular radius r_θ is computed in the same way for the four group samples considering just the galaxies with $|\Delta v_{l-o-s}| \leq 10^3 \text{ km s}^{-1}$ in each group. Just to give a quantitative comparison of the $2r_\theta$ defined in equation 2 with the definition of angular diameter θ_G used in Hickson (1982), we have checked with the 100 HCGs that the angular diameter θ_G is around 1.1 times larger than the angular diameter $2r_\theta$, specifically $\theta_G \approx [0.9 - 1.3] \times (2r_\theta)$.

In Figure 2, the distribution in the $2r_{\text{phy}}-z_{UV}$ plane shows the first differences between the compact group samples under comparison here. The SFCG sample presents a linear trend, relatively tight, in which the nearby SFCGs have much smaller sizes (less than 100 kpc diameters for $z < 0.05$) compared to the distant ones (more than 200 kpc diameters for $z > 0.1$). On the other hand, the HCG sample shows a more dispersed relation and the 2MCG presents a more restricted redshift range below $z \sim 0.05$ and a size range showing the

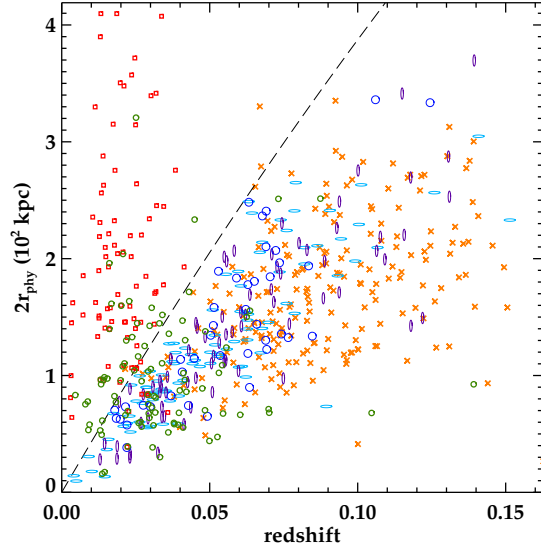


Fig. 2.— **Physical diameter $2r_{\text{phy}}$ versus redshift. Cyan horizontal and violet vertical ellipses correspond to those SFCGs with $m_z=1$ and $m_z=2$, respectively. Those SFCGs with $m_z \geq 3$ are represented by large blue circles. Small green circles, red squares and orange crosses correspond to the HCG, 2MCG and SCGA sample, respectively. Dashed line corresponds to an angular diameter of $2r_\theta=3.5$ arcmin.**

largest values in physical size. The SCGA sample shows one major concentration delimited by a redshift interval of $0.03 < z < 0.15$ and a physical size interval of $100 < (2r_{\text{phy}}/\text{kpc}) < 250$. The differences among group samples are probably due to the specific selection criteria applied to each sample and the original galaxy sample from which they were extracted, as explained below.

In the SFCG sample, the compactness criterion is applied over the projected galaxy-galaxy angular separations of the group members. This typically identifies groups of a similar or smaller angular size than the linking-length value of 1.5 arcmin, producing that, at a given angular size, distant groups have larger physical size as one can see in Fig. 2. By contrast, the compactness criterion of the HCG sample is applied over the total surface brightness of group members. This search criterion is fulfilled by galaxy groups along a sequence

Table 3: Comparison of significant percentiles values (Q_{16} , Q_{50} and Q_{84}) of redshift and physical size of SFCG, HCG, 2MCG and SCGA samples.

Sample ($m_z \geq 3$) (1)	Q_{16} (2)	Q_{50} (3)	Q_{84} (4)
z_g			
SFCG	0.0275	0.0622	0.0723
HCG	0.0145	0.0297	0.0485
2MCG	0.0126	0.0201	0.0290
SCGA	0.0615	0.0857	0.1211
$2r_{\text{phy}}$ (kpc)			
SFCG	73.2	133.7	196.5
HCG	57.9	89.0	144.8
2MCG	106.6	171.6	275.7
SCGA	111.4	164.7	236.4

Columns: (1) Acronym of each compact group sample, (2) 16-centile, (3) 50-centile and (4) 84-centile of the corresponding variables: z_g on the top and $2r_{\text{phy}}$ on the bottom.

in which the extremes are very compact groups of faint galaxies at one end and relatively more extended groups of bright galaxies in the other end. Knowing that in the $2r_{\text{phy}}-z_g$ diagram the angular size is represented by the slope of the trend, the dispersed relation of the HCG sample is explained the broader range of angular sizes found for the HCG sample.

The 2MCG sample presents a more restricted redshift range below $z \sim 0.05$ for being a velocity-filtered group sample mainly retrieved from the 2MASS Redshift Survey (Huchra et al. 2012) with a similar depth in redshift. Although the 2MCG sample is defined with the same compactness criterion, with a group K -band surface brightness threshold meant to match the R-band threshold of Hickson (1982), the 2MCGs are somewhat less compact. This can be explained by the known bias of the HCG sample towards high values of group surface brightnesses (Walke & Mamon 1989; Prandoni et al. 1994). The SCGA with $m_z \geq 3$ is extracted from the Main Galaxy Sample (MGS) of the Sixth Data Release (DR6, Adelman-McCarthy et al. 2008) of the Sloan Digital Sky Survey (SDSS); this explains that they are shar-

ing a similar redshift distribution $0.03 \lesssim z \lesssim 0.15$.

In Table 3, one can see that the 2MCG sample presents a distribution well concentrated around a median redshift of $\langle z \rangle = 0.02$, the HCG shows a bit more extended z -distribution with its significant percentiles ~ 1.15 - 1.67 higher than the corresponding 2MCG redshift percentiles. Differently, the SFCG and the SCGA samples show a clearly more extended redshift distribution with a median redshift of $\langle z \rangle = 0.062$ and $\langle z \rangle = 0.086$ greater than the 84-centile of the two other group redshift distributions. The SCGA sample is the least dispersed of the four samples, when dispersion is measured relative to the median.

On the other hand, the physical diameter distributions of the SFCG and HCG samples contain important fractions of groups that are more compact than 75 kpc in physical diameter $2r_{\text{phy}}$. In comparison with HCG sample, the SFCG sample contains an important part of the population which is more extended than 130 kpc in physical diameter $2r_{\text{phy}}$, increasing the median physical diameter to $\langle 2r_{\text{phy}} \rangle \sim 130$ kpc in comparison with the median physical diameter of the HCG sample, $\langle 2r_{\text{phy}} \rangle \sim 90$ kpc. Differently from the SFCG and the HCG samples, the 2MCG and the SCGA samples present a physical diameter distribution extending towards larger values, which is reflected in its higher percentiles compared to the two other group samples.

3.2. Ultraviolet colour distribution and comparison with other group samples

Figure 3 displays the GALEX colour-magnitude and color distributions for the SFCG, HCG, 2MCG and SCGA samples. In the four samples, the panels only show those group galaxies with a ultraviolet detection in the GALEX/AIS catalogue for both GALEX bands, FUV and NUV.

The panels of Figure 3 show three aspects of the colour distribution of the four samples of compact groups: the colour-magnitude diagram (top), the differential distribution of dereddened $(FUV-NUV)_d$ for the four group samples (middle) and the differential distribution of three subsets of the SFCG galaxy sample: galaxy members of SFCGs with $m_z \geq 3$, galaxy members of SFCGs with $m_z = 2$ and the non-member galaxies (bottom). The three panels of Figure 3 show the

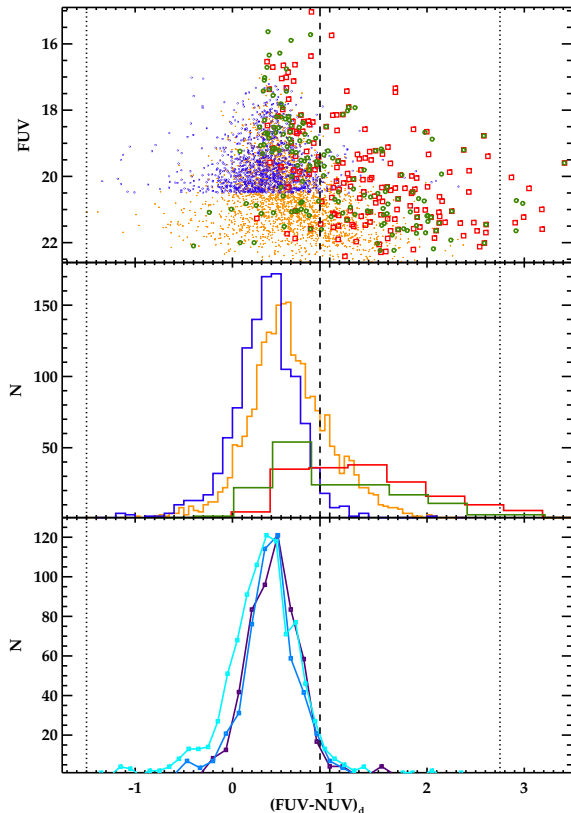


Fig. 3.— **Top panel:** Ultraviolet colour distributions of SFCG (blue), HCG (green), 2MCG (red) and SCGA (orange) samples. **Top panel:** FUV vs. $(FUV-NUV)_d$ for the four samples. The middle vertical dashed line corresponds to the FUV-NUV threshold between late-type and early-type galaxies proposed by Gil de Paz et al. (2007). The left and right vertical dotted lines delimit the colour constraint used in this work to retrieve ultraviolet sources from the GALEX/AIS catalogue. **Middle panel:** FUV-NUV color distributions of the four samples. Note that the histograms have different binning. **Bottom panel:** FUV-NUV color distributions of the subsets of galaxy members of SFCGs with $m_z \geq 3$ (violet), galaxy members of SFCGs with $m_z = 2$ (blue) and non-member galaxies (cyan). The three histograms are normalized to the maximum of the cyan histogram.

$(FUV-NUV)_d$ constraints included in the search strategy and described in Subsection 2.1 (left and right dotted vertical lines) and also the ultraviolet colour threshold (middle vertical dashed line) which segregates the late-types from early-type galaxies (Gil de Paz et al. 2007). Gil de Paz et al. (2007) find for a sample of nearby galaxies that the fraction of elliptical/lenticular galaxies with $(FUV-NUV)$ colour bluer than 0.9 mag (and both FUV and NUV magnitudes available) is 18%, while the percentage of spiral and irregulars redder than this value is only 12%.

Figure 3 clearly shows the limitation of optically and near-infrared selected group samples in finding groups dominated by star-forming galaxies, proving the interest of building a SFCG sample because of searching over ultraviolet catalogues. Inspecting Figure 3, one can see that virtually the entire ultraviolet colour distributions of the HCG, the 2MCG and the SCGA galaxies are within the $(FUV-NUV)_d$ constraints included in our search strategy (depicted by the left and right dotted vertical lines). This shows that the $(FUV-NUV)_d$ constraint is not the main responsible for rejecting from our search neither optically and/or near-infrared bright group galaxies nor early-type galaxies. In particular, the main limitation of those group galaxies to be retrieved by the search strategy described in this work is that they are not bright enough in the ultraviolet spectral range. In this respect, the compact group samples retrieved from the GALEX/AIS catalogue with the sole criterion of being detected in both GALEX bands correspond to 35% of the original HCG galaxy sample of 463 galaxies, 48% of the original 2MCG galaxy sample of 364 galaxies and 26% of the original SCGA galaxy sample of 9713 galaxies, the lowest fraction of the three samples. Once the $(FUV-NUV)_d$ colour, photometric quality flag and especially the FUV flux are considered in the compact group selection, these fractions are reduced from the previous 35% to 19% for the HCG galaxy sample, from the previous 48% to 25% for the 2MCG galaxy sample and from the previous 26% to 11% for the SCGA galaxy sample, which is again the lowest fraction of the three samples. Table 4 summarizes the fractions described above for the four samples under comparison in this work.

On the other hand, among the galaxies that

Table 4: Fractions characterizing the GALEX UV magnitude and color distribution of the group galaxy population for each group sample.

Sample	FUV&NUV	UV bright	UV blue
(1)	(2)	(3)	(4)
SFCG	100	100	96
HCG	35	19	53
2MCG	48	25	28
SCGA	26	11	79

Columns: (1) Acronym of each compact group sample, (2) fraction of group galaxies detected in both GALEX bands, (3) fraction of group galaxies detected in both bands which fulfill the GALEX constraints used to select SFCG galaxies and (4) fraction of group galaxies detected in both bands bluer than $FUV-NUV=0.9$.

are detected in both FUV and NUV wavebands of GALEX in the other three compact group samples, significant fractions are bluer than the ultraviolet colour cut proposed by Gil de Paz et al. (2007): 53%, 28% and 79% for the HCG, the 2MCG and the SCGA samples, respectively (see the bottom panel of Fig. 3). Nevertheless, these very blue galaxies are relatively less frequent in these three reference compact group samples than they are in the SFCG sample (96%), and the median $FUV-NUV$ is also well redder than median ultraviolet colour $\langle FUV-NUV \rangle = 0.351$ of the SFCG sample: $\langle FUV-NUV \rangle = 0.803$ for the HCG sample $\langle FUV-NUV \rangle = 1.323$ for the 2MCG sample and $\langle FUV-NUV \rangle = 0.550$ for the SCGA sample (see table 5).

In the bottom panel of Fig. 3, it is also displayed the UV colour distributions of galaxy members of SFCGs with $m_z \geq 3$ (violet lines), $m_z = 2$ (blue lines) and also for the non-member galaxies (cyan lines) with the aim of checking the presence of a population of interlopers with a different ultraviolet colour distribution.

A Kolmogorov-Smirnov test applied to the $m_z = 2$ and $m_z \geq 3$ UV color distributions produces a probability of 32% that the two colour distributions come from the same parent population. The same test applied between the UV color distribu-

Table 5: Comparison of significant percentiles values (Q_{16} , Q_{50} and Q_{84}) of UV colors of SFCG, three subsamples of the former sample, HCG, 2MCG and SCGA samples.

$(FUV-NUV)_d$				
Sample	Q_{16}	Q_{50}	Q_{84}	N
(1)	(2)	(3)	(4)	(5)
SFCG	0.048	0.351	0.652	1193
$m_z \geq 3$	0.180	0.421	0.669	128
$m_z = 2$	0.146	0.369	0.635	148
non-membs	0.014	0.332	0.652	904
HCG	0.406	0.803	1.853	162
2MCG	0.649	1.323	2.123	174
SCGA	0.208	0.550	0.990	2517

Columns: (1) Acronym of each compact group sample, (2) 16-centile, (3) 50-centile, (4) 84-centile of the $(FUV-NUV)_d$ distribution and (5) the total number of galaxies detected in both GALEX bands.

tions of the non-member population and the $m_z = 2$ population gives a 1.3% probability whereas this test gives a 0.01% probability between the non-member population and the $m_z \geq 3$ population. Therefore, the non-member population is statistically distinguishable from the $m_z = 2$ and $m_z \geq 3$ populations, which are very similar between them. This fact can be also observed in the bottom panel of Fig. 3 and the second and third rows of Table 5 in the comparison of the UV color distributions of these three SFCG subsamples where there is an extra population of galaxies with $FUV-NUV \lesssim 0$ in the subsample of non members.

To analyse the origin of this extra population having $FUV-NUV \lesssim 0$ in the non-member subsample, we have computed the k-correction using the calculator provided by Chilingarian & Zolotukhin (2012)². We computed the difference between the observed GALEX colour $(FUV-NUV)_{obs}$ and the rest-frame GALEX colour $(FUV-NUV)_{r-f}$ as a function of redshift for blue galaxies i.e:

²<http://kcor.sai.msu.ru>

$$\begin{aligned}
& (\text{FUV}-\text{NUV})_{\text{obs}} - (\text{FUV}-\text{NUV})_{\text{r-f}} = \\
& = -[k_{\text{FUV}}(z; \text{color}_1) - k_{\text{NUV}}(z; \text{color}_2)]. \quad (3)
\end{aligned}$$

The k-correction $k_\lambda(z; \text{color}_i)$ is defined as $k_\lambda(z; \text{color}_i) = m_{\text{r-f}} - m_{\text{obs}}(z)$. The k-correction is applied to the FUV band taking a GALEX color for blue galaxies of $\text{color}_1 \equiv \text{FUV}-\text{NUV} \sim 0.35$ (see Fig. 3) and the k-correction is applied to the NUV band assuming a SDSS-GALEX color for blue galaxies of $\text{color}_2 \equiv \text{NUV}-r' \sim 2$ (c.f. Hernández-Fernández et al. 2012). We find that the $(\text{FUV}-\text{NUV})_{\text{obs}}$ of blue galaxies as a function of redshift only goes bluer than the $(\text{FUV}-\text{NUV})_{\text{r-f}}$ for redshifts above $z \sim 0.1$. This suggests that the bluest FUV-NUV colours are indeed caused by galaxy interlopers or also galaxy groups at $z > 0.1$.

Comparing the 16-centiles of the UV color distributions of the SFCG subsets, $m_z \geq 3$, $m_z = 2$ and non-members (see Table 5), we should note that the 16-centile of the non-member galaxy sample $Q_{16} = 0.014$ is clearly lower than the other two subsets, $Q_{16} = 0.146$ for $m_z \geq 3$ and $Q_{16} = 0.180$ for $m_z = 2$. This suggests that interlopers play a role in producing even bluer median colors, but that this effect $Q_{50}(\text{SFCG}) - Q_{50}(m_z \geq 3) = -0.07$ is much smaller than the difference in median colors with the 2MCG, HCG and SCGA samples, $Q_{50}(\text{SCGA}) - Q_{50}(m_z \geq 3) = 0.129$ in the worst case.

3.3. Results from an ultraviolet search over the galaxy catalogue of HCG sample

With the aim of comparing the approach of identifying galaxy groups using catalogues of UV emitting galaxies with the approach of searching groups in catalogues of optically and near-infrared selected galaxies, we apply the same methodology described in this work over the sample of group galaxies from the HCG catalogue (Hickson et al. 1992) consisting of 463 galaxies. We take the HCG sample as the prototype of the optically or near-infrared selected group samples, assuming that similar results should be expected for others (e.g. Prandoni et al. 1994; Barton et al. 1996; Díaz-Giménez et al. 2012). The test provides the following results:

- From a total of 463 HCG galaxies, only 87 galaxy members fulfill the constraints on

FUV brightness, UV colour and GALEX photometric quality. This means that on average, the HCG sample contains less than one UV-bright galaxy per group.

- Specifically, only three HCGs have four or more HCG galaxy members fulfilling the GALEX UV constraints: HCG23, HCG89 and HCG100 with four UV-bright galaxy members in each of them. This low ratio (3%) points out the main limitation of the HCGs to be included in a sample of SFCGs; they are mainly populated by galaxies without a bright UV counterpart.
- Furthermore, there are no HCGs with four or more UV-bright members and also fulfilling our compactness criterion: a maximum angular distance of 1.5 arcmin from each member to some of the rest of HCG galaxy members.
- The output of this test just gives HCG100 as a compact group of UV-bright galaxies but only with three UV-bright members close enough. Then, HCG100 should not be in principle included in the SFCG sample. However, HCG100 (identified here as SFCG2) does belong to the sample of SFCGs because there is a fourth UV-bright galaxy not in the HCG catalogue, which lies ≈ 1 arcmin to the Southeast of HCG100b (denoted HCG100x by Plana et al. 2003)³. This galaxy HCG100x is therefore a member of the selected SFCG, while the HCG member HCG100c does not fulfill the compactness criterion applied in this work, a maximum angular separation of 1.5 arcmin (see the corresponding image in the stamp collection).
- We note that there is one of the HCG sample that deserves maintaining in this context as an extreme case, the system HCG54. This system has been considered to be a single galaxy rather than a group (Verdes-Montenegro et al. 2002; Torres-Flores et al. 2010). HCG54 is identified as one single UV source by the GALEX photometric code.

³The celestial coordinates of this object are R.A.=01:29:52, Dec.=13:05:54.9

3.4. Kinematical analysis and comparison with other group samples

Figure 4 shows results of a kinematical analysis of the subset of SFCGs with more than three members (top panel, three members $m_z=3$ and bottom panel, four members $m_z=4$). This comprises 36 groups with $m_z=3$ and 5 groups with $m_z=4$. Instead of showing the distribution of l-o-s velocities with respect to the median redshift i.e. Δv_{1-o-s} , we show the velocity distribution with respect to the average redshift $\langle z_{\text{memb}} \rangle$ of the m_z galaxy members i.e.:

$$\Delta v_{\text{memb}} = c \left(\frac{z_{\text{memb}} - \langle z_{\text{memb}} \rangle}{1 + \langle z_{\text{memb}} \rangle} \right). \quad (4)$$

This avoids the artifact of a central peak with $\Delta v_{1-o-s}=0$. The solid lines depict the normal distributions derived from the maximum likelihood fitting, i.e. by minimizing

$$-\ln \mathcal{L} = -\sum_i \ln p_i, \quad (5)$$

where $\mathcal{L} = \prod_i p_i$ is the likelihood,

$$p_i = \frac{1}{\sqrt{2\pi}\sigma^2} \exp \left[-\frac{(\Delta v_{\text{memb}} - \mu)^2}{2\sigma^2} \right], \quad (6)$$

and where Δv_{memb} is the velocity offset of galaxy i and μ is the mean velocity offset from the group mean velocities. Naturally, it makes no sense to consider non-zero mean velocity offsets from the group mean velocities, so we simplify to $\mu=0$. The dashed lines show the normal distributions fixed to the standard deviation directly derived from the Δv_{memb} distribution. The dotted lines show the normal distributions fixed to the median velocity dispersion of the corresponding subsample.

The derived values of l-o-s velocity dispersion for those $m_z=3$ SFCGs are in the range of $\sigma_{1-o-s} \approx 135-170 \text{ km s}^{-1}$ which contains the median velocity dispersion of the spiral-rich HCGs ($\sigma_{1-o-s} \approx 140 \text{ km s}^{-1}$) but it is clearly lower than the median σ_{1-o-s} of the spiral-poor HCGs ($\sigma_{1-o-s} \gtrsim 250 \text{ km s}^{-1}$, Hickson 1997). In the case of SFCGs with $m_z=4$, the derived values of l-o-s velocity dispersion are in the range of $\sigma_{1-o-s} = 155-200 \text{ km s}^{-1}$ which is closer to the median σ_{1-o-s} of

the spiral-rich HCGs (Hickson 1997, fig. 3). The fact that the typical SFCG velocity dispersion is closer to that of the spiral-rich HCGs (Hickson 1997) is in agreement with the high fraction of late-type galaxies expected from the FUV–NUV colours shown by the SFCG galaxy sample i.e. $\text{FUV} - \text{NUV} \lesssim 0.9$.

The top panel of Figure 5 shows the distribu-

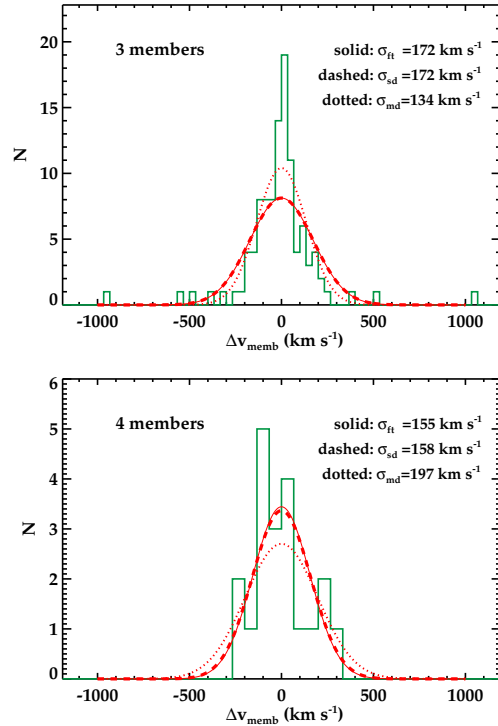


Fig. 4.— Distributions of line-of-sight velocities (relative to the group mean) of the subset of SFCGs with $m_z=3$ (top panel) and $m_z=4$ (bottom panel). Solid curves are fits to the stacked distribution of velocities relative to the group mean velocity. Dashed and dotted curves show the normal distributions with standard deviations equal to that of the Δv distribution and to the median of the standard deviations, respectively. The l-o-s velocity dispersion values derived from the fitting σ_{fit} , from the standard deviation of the Δv_{memb} distribution σ_{sd} and the median velocity dispersion of the corresponding subsample σ_{md} are shown at the upper left region of each panel.

tion of the median projected physical separations R_{ij} with respect to the velocity dispersion σ_{1-o-s} for the sample of SFCGs (blue empty circles), the HCG sample (green points), the 2MCG sample (red squares) and the SCGA sample (orange crosses). The median projected physical separation R_{ij} is computed as the median physical length of the two-dimensional galaxy-galaxy separation vectors of the galaxy members for the SFCGs, HCGs and SCGAs with $m_z \geq 3$. The R_{ij} values of the 2MCG sample are translated from the original work (Díaz-Giménez et al. 2012) to the cosmological model used in this work. The top panel also includes the four linear fits in the log-log plane of these variables i.e.:

$$\log(R_{ij}/\text{kpc})_{\text{fit}} = A \log(\sigma_{1-o-s}/\text{km s}^{-1}) + B.$$

The parameter values derived from these linear fits and their associated uncertainties are shown in Table 6.

Table 6: **Derived parameters from linear fitting in the $\log(R_{ij})$ vs. $\log(\sigma_{1-o-s})$ plane.**

Sample	$A \pm \delta A$	$B \pm \delta B$
(1)	(2)	(3)
SFCG	-0.021 ± 0.100	1.92 ± 0.21
HCG	0.050 ± 0.082	1.65 ± 0.19
2MCG	-0.058 ± 0.086	2.18 ± 0.20
SCGA	-0.055 ± 0.036	2.162 ± 0.082

Columns: (1) Acronym of each compact group sample, (2) logarithmic slope and (3) ordinate at the origin of the linear fit
 $\log(R_{ij}/\text{kpc})_{\text{fit}} = A \log(\sigma_{1-o-s}/\text{km s}^{-1}) + B.$

The top panel of Figure 5 shows clearly that the different group samples present comparatively distinct size averages for any given velocity dispersion. Despite the four group samples are distributed in a similar range of R_{ij} , $20 \lesssim (R_{ij}/\text{kpc}) \lesssim 200$, their medians (see Table 7) show distinct values: $R_{ij} \sim 80$ kpc for the SFCGs, $R_{ij} \sim 60$ kpc for the HCG and $R_{ij} \sim 110$ kpc for the 2MCG and SCGA. Further, the linear fits $\log(R_{ij})$ vs. $\log(\sigma_{1-o-s})$ presents a negligible slope within uncertainties (see Table 6). This fact can be interpreted as an effect of the selection of groups in projection which is not biased toward any of the situations characterizing groups selected in projection: physically rounded groups, groups physically

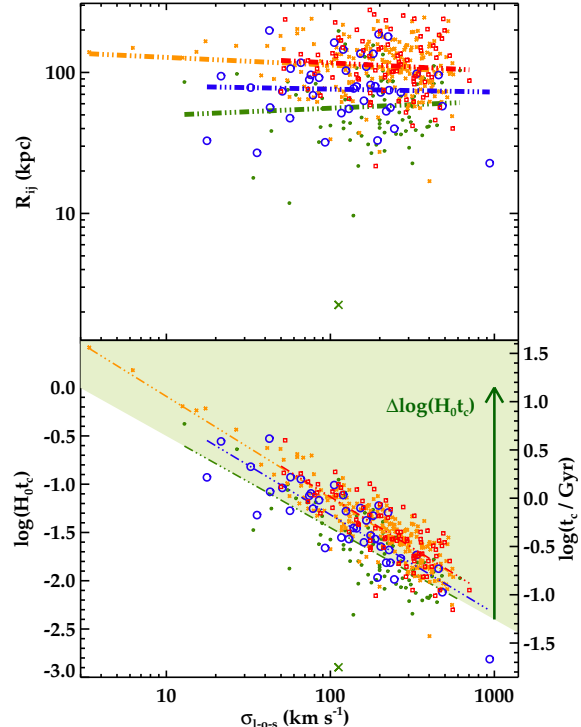


Fig. 5.— Blue empty circles, green points, red squares and orange crosses correspond to the SFCG, HCG, 2MCG and SCGA samples, respectively. HCG54 is depicted by a green cross at the bottom of each panel. Linear fits for each sample is shown with the same color code. Top panel: Median projected physical separation vs. 1-o-s velocity dispersion. Bottom panel: Crossing time vs. 1-o-s velocity dispersion. The crossing time t_c is shown in dimensionless (left axis) and physical (right axis) units. Green shaded area delimits the diagram space where $\Delta \log(H_0 t_c)$ (see Eq. 8) is considered positive in the increasing direction indicated by the vertical green arrow.

elongated along the line-of-sight direction or also chance galaxy alignments along the line-of-sight direction. The predominance of each one of these situations has been analysed by Díaz-Giménez & Mamon (2010).

We should add that, according to the median values of velocity dispersion and median projected physical separation of the four compact group

samples given in Table 7 and assuming the virial condition i.e $M_{\text{vir}} \propto \sigma^2 R_{ij}$ where M_{vir} corresponds to the virial theorem mass of the system, the virial theorem masses of SFCGs are on average 1.6, 4.2 and 3.8 times lower than the HCG, 2MCG and SCGA samples, respectively.

Table 7: **Comparison of significant percentiles values (Q_{16} , Q_{50} and Q_{84}) of velocity dispersion, crossing time and median projected physical separation of SFCG, HCG, 2MCG and SCGA samples.**

Sample ($m_z \geq 3$) (1)	Q_{16} (2)	Q_{50} (3)	Q_{84} (4)
σ_{1-o-s} (km s ⁻¹)			
SFCG	51.0	138.7	228.0
HCG	89.1	204.2	323.6
2MCG	108.0	241.0	391.0
SCGA	100.3	227.1	340.0
$\log(H_0 t_c)$			
SFCG	-1.81	-1.33	-1.04
HCG	-2.03	-1.78	-1.33
2MCG	-1.82	-1.55	-1.09
SCGA	-1.82	-1.48	-1.13
R_{ij} (kpc)			
SFCG	47.4	78.1	117.2
HCG	36.3	58.7	94.5
2MCG	68.4	108.3	180.3
SCGA	72.3	111.5	157.9

Columns: (1) Acronym of each compact group sample, (2) 16-centile, (3) 50-centile and (4) 84-centile of the corresponding variable: σ_{1-o-s} on the top, $\log(H_0 t_c)$ in the middle and R_{ij} on the bottom.

Figure 5 also shows in its bottom panel the relation of the crossing-time t_c with respect to the l-o-s velocity dispersion σ_{1-o-s} (bottom panel) for the four samples. The crossing-time is defined as:

$$t_c = \frac{\pi}{2} \frac{R_{ij}}{\sqrt{3} \sigma_{1-o-s}}. \quad (7)$$

The crossing time values from the 2MCG sample are translated to the cosmological model used in this work whereas the crossing time values of the SFCG, HCG and SCGA samples are computed with the very same cosmological model and with the crossing time formula given in Equation

7. The bottom panel of Figure 5 also displays the linear fits in the log-log plane i.e.

$$\log(H_0 t_c)_{\text{fit}} = M \log(\sigma_{1-o-s}/\text{km s}^{-1}) + N,$$

to the four samples. The parameter values derived from these linear fits and their associated uncertainties are shown in Table 8. The linear fit to the HCG sample does not include the HCG54 with a crossing time value $\log(H_0 t_c) \approx -2.9$ because it is showing a clear outlier behaviour and it is considered a galaxy remnant and not a galaxy group (Verdes-Montenegro et al. 2002; Torres-Flores et al. 2010).

Table 8: **Derived parameters from linear fitting in the $\log(H_0 t_c)$ vs. $\log(\sigma_{1-o-s})$ plane.**

Sample (1)	$M \pm \delta M$ (2)	$N \pm \delta N$ (3)
SFCG	-1.021 ± 0.100	0.73 ± 0.21
HCG	-0.950 ± 0.083	0.45 ± 0.19
2MCG	-1.056 ± 0.087	0.98 ± 0.20
SCGA	-1.055 ± 0.036	0.964 ± 0.082

Columns: (1) Acronym of each compact group sample, (2) logarithmic slope and (3) ordinate at the origin of the linear fit $\log(H_0 t_c)_{\text{fit}} = M \log(\sigma_{1-o-s}/\text{km s}^{-1}) + N$.

The linear fits in Fig. 5 present similar slopes for the four samples and they are close to minus one within uncertainties. If the fitted slopes are not affected by incompleteness in the plane $\log(H_0 t_c) - \log(\sigma_{1-o-s})$, this coincidence of $M \approx -1$ means that the projected physical sizes of compact groups in these samples would not present a significant trend with velocity dispersion and it can be seen also in the top panel of Figure 5. This is contrary to one would expect for a galaxy system assuming a principle of homology.

On the other hand, the 2MCG and SCGA samples, which share a very similar trend in the $\log(H_0 t_c)$ vs. $\log(\sigma_{1-o-s})$ plane, present systematically longer crossing times than the SFCG sample and the SFCG sample shows systematically longer crossing than the HCG sample, for a given velocity dispersion. This places the four group samples in an evolutionary sequence from a dynamical point of view, in which the HCG sample is the more dynamically evolved group sample and the SFCG sample is in an intermediate stage be-

tween the HCGs at one end, and the 2MCG and SCGA samples in the other end, being these ones less dynamically evolved.

Specifically, for given group velocity dispersion, the typical crossing time of the SFCG sample with respect to the HCG linear fit (i.e. $\log(H_0 t_c)^{\text{HCG}}$) is on average 36% longer i.e. $\Delta \log(H_0 t_c) = 0.13$, where we define $\Delta \log(H_0 t_c)$ as:

$$\Delta \log(H_0 t_c) = \log(H_0 t_c) - \log(H_0 t_c)^{\text{HCG}}_{\text{fit}}. \quad (8)$$

This crossing time increase reaches up to a 100% (i.e. $\Delta \log(H_0 t_c) = 0.30$) for the 2MCG and the SCGA samples with respect to the HCG sample.

For the SFCGs, the larger crossing times with respect to the HCG sample can be interpreted as an indication of less dynamically evolved groups and therefore, that their galaxies have been less affected by galaxy-galaxy interactions and environmental processes linked to the intragroup plasma and the dark matter group halo. This would allow the presence of a significant pristine gas reservoir in group galaxies and consequently such abundance of star-forming galaxies in the SFCGs. This does not seem to be the situation for the 2MCG and the SCGA samples as these groups have been extracted from near-infrared and optical selected galaxy catalogues respectively and, as shown in Subsections 3.2 and 3.3, the 2MCG and the SCGA samples should be poorly populated by star-forming galaxies. We outline a comprehensive explanation for both situations. Galaxy groups can be assembled from a mixture of previously passive and/or previously star-forming galaxies. Group searches in the near-infrared and optical catalogues are finding those groups mainly assembled from passive galaxies whereas the searches in ultraviolet catalogues are finding those groups mainly assembled from previously star-forming galaxies which still retain a significant amount of fresh gas. The evolutionary scenario previously described is graphically summarized in Figure 6.

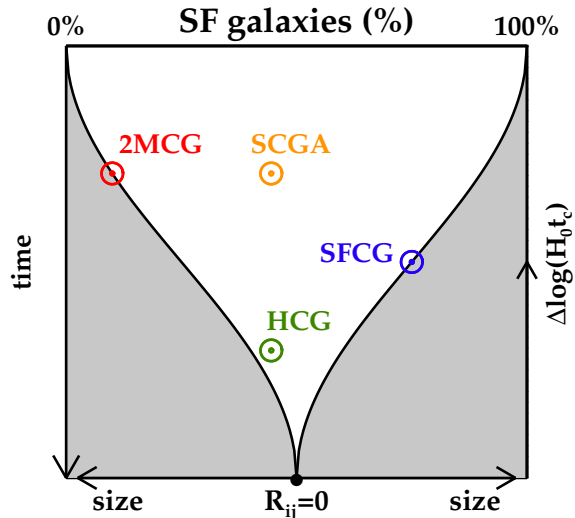


Fig. 6.— Scheme which summarizes and compares the typical characteristic evolutionary stage, fraction of star-forming galaxies and physical size of the three group samples compared here. The vertical axis depicts an evolutionary sequence (left axis) in which the proxy is considered the surplus in crossing time with respect to the HCG linear fit $\Delta \log(H_0 t_c)$ (right axis), see Eq. 8. The horizontal axis attempts to account for the star-forming fraction of galaxy members at the top of the graph and, the evolution of the physical size of the galaxy groups along cosmic time, at the bottom.

4. Cross-matching with compiled catalogues of galaxies, groups and galaxy clusters

4.1. Search for analogues of BIG

With the aim of finding analogues to the Blue Infalling Group, the better known example of a SFCG infalling to a cluster (ABELL 1367), we cross-matched the sample of SFCGs with the largest compilation of catalogues of galaxy clusters, NED (NASA/IPAC Extragalactic Database). We searched for objects compiled by NED as galaxy clusters (“GClust”) up to a searching radius of 50 arcmin. We set the upper redshift to $z=0.3$, noting that the highest values of SFCG

redshifts are around $z \sim 0.15$. Figure 7 shows the distribution of the resulting SFCG-cluster matches in projected physical separation D_{sep} in Mpc, and line-of-sight velocity difference Δv , with respect to the candidate parent cluster. Note that both cluster virial radii and/or velocity dispersions are not known or computed for every cluster compiled by NED.

The precise definition of the infalling regions in the cluster projected phase has been recently studied (e.g. Mahajan et al. 2011; Haines et al. 2012; Oman et al. 2013) and always suffers of overlapping problems because a six-dimensional phase space is being collapsed into a two dimensional projected phase space. Because of these limitations, we just tentatively identify as infalling groups those that are sufficiently close to the parent cluster i.e.:

$$D_{\text{sep}} < 1 \text{ Mpc AND } 1000 < \left(\frac{|\Delta v|}{\text{km s}^{-1}} \right) < 2000$$

OR

$$1 < \left(\frac{D_{\text{sep}}}{\text{Mpc}} \right) < 3 \text{ AND } |\Delta v| < 1000 \text{ km s}^{-1}$$

but excluding the cluster central regions:

$$D_{\text{sep}} < 1 \text{ Mpc AND } |\Delta v| < 1000 \text{ km s}^{-1}.$$

Within these boundaries, we find 26 SFCGs embedded in the infall regions of 32 candidate parent clusters. Note that a few of the SFCGs are embedded in the infall regions of more than one cluster. We also find 31 SFCGs in the central regions of clusters. In this cluster central region, most of the SFCGs should be identified with the cluster itself.

4.2. Cross-matching with catalogues of galaxy groups and galaxies

4.2.1. Cross-matching with catalogues of known galaxy groups

In order to know whether there is a previously identified galaxy group at the sky position of each SFCG, we tentatively crossmatch the sample with those objects classified by NED as galaxy clusters (“GClust”) or galaxy groups (“GGroup”) inside a searching radius of 6 arcmin. Knowing that the linking length in the FoF algorithm is set to a maximum of 1.5 arcmin, we can assume that a searching radius of 6 arcmin is enough to find a galaxy group counterpart for each SFCG, if it exists. The redshifts (when available) of NED groups are con-

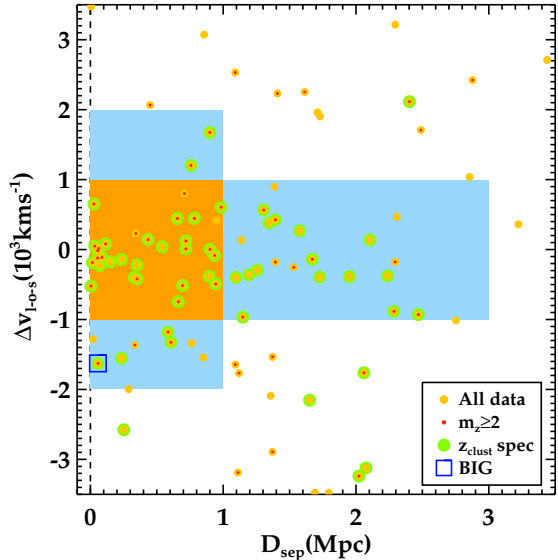


Fig. 7.— Stack of projected phase space diagram of SFCGs with respect to their candidate parent cluster, Δv vs. D_{sep} . The red points represent those groups with $m_z \geq 2$. Green large circles mark those groups where the redshift of the candidate parent cluster is spectroscopically-derived indicating an accurate cluster redshift. The BIG is labeled by a blue square. Those groups tentatively identified as infalling groups are those ones located over the blue shaded area while the groups considered as groups located in the central region of clusters are those ones located over the orange shaded area.

sidered as additional estimates for the matching SFCGs.

As can be seen in the three panels of Figure 8, two sets of crossmatched group pairs are clearly distinguishable, those with velocity differences lower than $|\Delta v| \sim 1000 \text{ km s}^{-1}$ and those with larger velocity differences. Inspecting the subset with large velocity differences, we note that there are six examples of galaxy groups with more robust group redshifts z_{UV} i.e. $m_z \geq 2$. These ones correspond to the red and orange data circles with a central black point in Fig. 8. A first characteristic of this subset (all in the upper right portion of the middle panel of Figure 8) is that it presents groups with large separations ($D_{\text{sep}} > 3.5 \text{ arcmin}$),

suggesting that there is no physical connection between the SFCG and the previously catalogued group. This is confirmed by the $D_{\text{sep}}/r_{\theta}$ values (see Table 9 and bottom panel in figure 8) which show that the centers of the NED groups lie more than three SFCG group radii away from these SFCG groups and in consequence, clearly outside from the physical extension of the SFCG. These groups and their corresponding NED group counterparts are shown in Table 9 and they are described in detail in the following:

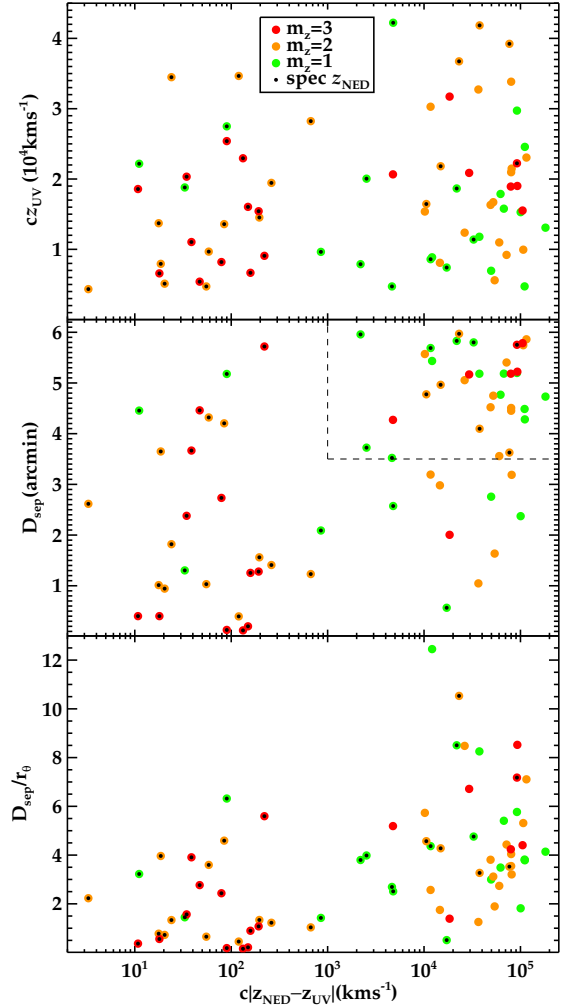


Fig. 8.— Diagnostics of matches between SFCGs and NED group/clusters of known redshift in terms of absolute l-o-s velocity difference. *Top*: l-o-s velocity of SFCGs. Colour code identifies the numbers of known UV-galaxy redshifts to define the SFCG redshift. The black points mark those CSGFs where the redshift of the NED group is spectroscopically-derived. *Middle*: Angular separation. The two dashed lines at $|\Delta v|=1000 \text{ km s}^{-1}$ and $D_{\text{sep}}=3.5 \text{ arcmin}$ indicate those groups with large velocity differences and separation distances, respectively (see text for details). *Bottom*: Angular separation in units of SFCG size r_{θ} .

Table 9: SFCGs with large velocity differences and large separations with respect to their known group counterparts.

n_{ID}	Object Name	z_{NED}	Δv km s ⁻¹	RA deg	Dec deg	D_{sep} arcmin	r_{θ} arcmin
(1)	(2)	(3)	(4)	(5)	(6)	(7)	(8)
92	SDSSCGB 46521	0.3810	91986	161.708	43.0632	5.7	0.801
106	WBL 340	0.0196	-10560	173.910	54.8901	4.8	1.045
117	ABELL 1514	0.1995	23074	184.484	20.6542	6.0	0.567
134	[RPG97] 236	0.0232	-14864	198.638	17.1708	5.0	1.160
146	SDSSCGB 49472	0.3870	76793	206.894	32.5728	3.6	1.029
256	UGCl 314	0.0139	-37688	211.808	12.6627	4.1	1.253

(1) ID number of the SFCG, (2) NED object name of group counterpart, (3) NED redshift of group counterpart, (4) Velocity difference between the SFCG and its group counterpart, (5) and (6) celestial coordinates of group counterpart, (7) separation distance on the sky between the SFCG and its group counterpart and (8) angular radius of the SFCG computed following Eq. 2.

- SFCG092: Although, SDSSCGB 46521 is separated from this SFCG by $D_{\text{sep}}=5.8$ arcmin, there is another closer ($D_{\text{sep}}=0.3$ arcmin) group (SDSSCGA 01937) with unknown redshift that may or may not be associated to it.
- SFCG106: WBL 340 is its closer counterpart with $D_{\text{sep}}=4.8$ arcmin and it is clearly not physically linked to it. However, from the study presented in section 4.1, we know that this SFCG is embedded in a larger structure, ABELL 1318.
- SFCG117: ABELL 1514 is separated from the SFCG117 by $D_{\text{sep}}=5.97$ arcmin. The nearest group to SFCG117 is a four-member galaxy group SDSSCGB 62865 without known redshift ($D_{\text{sep}}=3.948$ arcmin) which is also clearly separated from the SFCG.
- SFCG134: [RPG97] 236, this a three-member galaxy group with $D_{\text{sep}}=4.964$ arcmin.
- SFCG146: SDSSCGB 49472, this SDSS group is clearly separated from SFCG146 by a $D_{\text{sep}}=3.627$ arcmin.
- SFCG256: UGCl 314, the spectroscopic redshift of this cluster was derived from just one galaxy redshift in projection ($D_{\text{sep}}=4.097$ arcmin) of a previously identified Uppsala cluster.

In these examples, the matched groups are clearly not related to the SFCG, therefore the 6 arcmin matching radius was somewhat too liberal. From this fact together with the inspection of the SFCGs in the GALEX and optical images, shown in the collection of stamps cited at the end of section 2, we conclude that a crossmatching radius of 2.5 arcmin is an appropriate constraint to link a newly identified SFCG with a previously known galaxy group. Applying this constraint we find 59 SFCGs with a previously known group counterpart, 24 of which have known spectroscopic redshifts.

4.2.2. Search for group members without a bright UV counterpart

We are also interested in finding other UV-faint galaxies with known redshifts in the neighborhood

of each SFCG, particularly for those SFCGs with no redshift information. We derive a new additional redshift estimation with the same prescription that we applied for defining a redshift estimation for the set of UV galaxies belonging to each SFCG (see Subsection 2.4), but now we include all galaxies, UV-bright or not, within 2.5 arcmin from the SFCG center. The values for $\langle z_{\text{gal}} \rangle$ correspond to the median redshift among those galaxies with known redshifts inside a searching circle of $D_{\text{sep}}=2.5$ arcmin. The g_z is the number of galaxies with known redshift within a velocity interval of $|\Delta v_{1-o-s}| \leq 10^3 \text{ km s}^{-1}$ where Δv_{1-o-s} is the l-o-s velocity difference with respect to the redshift $\langle z_{\text{gal}} \rangle$. If there is no known redshift associated to the galaxies of a specific SFCG, we label the redshift value with zero, $\langle z_{\text{gal}} \rangle=0$. The derived group redshifts $\langle z_{\text{gal}} \rangle$ are shown in Table 10 and the overall set of compiled galaxy redshifts is also overplotted in the collection of stamps provided in Figure A1 of Appendix. This approach yields 222 group redshifts $\langle z_{\text{gal}} \rangle$ (79% of the whole sample) with 87 SFCGs with $g_z=1$ ($\approx 31\%$) and 135 SFCGs with two or more redshifts (48%). To summarize, we provide three redshift estimations for the SFCGs:

- z_{UV} defined by the UV-bright galaxies of the SFCG in Table 1,
- z_{NED} the NED redshift for a previously catalogued galaxy group in a neighbourhood of 2.5 arcmin in radius of the SFCG in Table 10 and,
- $\langle z_{\text{gal}} \rangle$ defined by the median of those galaxy redshifts found in a SFCG neighbourhood of 2.5 arcmin in radius in Table 10.

Table 10: Additional redshift counterparts

nID	$\langle z_{\text{gal}} \rangle$	g_z	z_{NED}	D_{sep} arcmin	Group Name
(1)	(2)	(3)	(4)	(5)	(6)
1	0	0	0	0	X
2	0.017899	3	0.017800	1.497	HCG_100
3	0.041719	1	0	0	X
4	0	0	0	0	X
5	0	0	0	0	X
6	0	0	0	0	X
7	0.093258	1	0	0	X
8	0.013066	2	0	0	X
9	0.036399	2	0	0	X
10	0.051799	1	0	0	X
11	0.093101	2	0	0	X
12	0.019557	2	0	0	X
13	0.041095	1	0	0	X
14	0.077190	4	0.077000	0.120	SDSSCGA_00909
15	0.063567	3	0.063600	1.409	ABELL_2800
16	0.086353	1	0	0	X
17	0	0	0	0	X
18	0.159397	1	0	0	X
19	0	0	0	0	X
20	0.041299	2	0	0	X
...
261	0.051225	4	0.050800	1.280	MCXC_J1749.8+6823
262	0.046689	1	0	0	X
263	0.055402	2	0	0	X
264	0	0	0	0	X
265	0	0	0	0	X
266	0.031292	1	0	0	X
267	0	0	0	0	X
268	0	0	0	0	X
269	0.070699	4	0	0	X
270	0	0	0	0	X
271	0.027636	2	0	0	X
272	0.017462	2	0.015960	0.913	WBL_178
273	0.069071	6	0	0	X
274	0.045465	2	0	0	X
275	0.085412	4	0.085000	0.129	SDSSCGA_00370
276	0.067000	2	0	0	X
277	0	0	0	0	X
278	0.000907	1	0	0	SDSSCGB_67914
279	0.063227	1	0.434700	0.579	WHL_J130719.4+133902
280	0.039417	1	0	0	X

(1) ID number of the SFCG, (2) median redshift for galaxies with known redshift given by NED inside $D_{\text{sep}}=2.5$ arcmin, (3) number of galaxies to derive the redshift, (4) NED group redshift, (5) angular separation distance between the SFCG and the previously identified galaxy group and (6) preferred NED name of a previously identified group counterpart.

4.3. Purity of the sample of SFCGs: Check of the projected and kinematical surroundings of SFCGs

Groups of galaxies selected in projection without the use of redshifts are subject to contamination by discordant-redshift galaxies. Díaz-Giménez & Mamon (2010) studied the purity of a sample of compact groups selected with the Hickson’s criteria from the $z=0$ output of three semi-analytical models of galaxy formation run on the Millennium Simulation. Among the “complete sample of compact groups fulfilling the Hickson’s criteria, roughly 60% of their different mock projected compact group samples have at least four galaxies within 10^3 km s^{-1} of the median velocity of the group.

Also, Mendel et al. (2011) found that when compact groups are selected according to the criteria of Hickson (1982), roughly half of the compact groups can be associated with relatively rich structures, while the remaining half are likely to be either independent structures in the field or associated with comparably poor groups.

With the same aim of estimating the fraction of SFCGs that present a minimum number of their galaxies with accordant l-o-s velocities, we retrieve all those objects with spectra classified as ‘galaxy’ in a radius of 15 arcmin around each group from the 10th Data release of the Main Galaxy Sample (MGS) of the Sloan Digital Sky Survey (SDSS). There are 139 groups compiled with good SDSS/MGS coverage. Among the 321 UV group members from the SFCG sample with a SDSS/MGS counterpart, there are 308 objects (i.e. 96%) spectroscopically classified as galaxies (**class**=‘GALAXY’), 4 UV members (i.e. 1.2%) classified as stellar objects (**class**=‘STAR’) and 9 objects (i.e. 2.8%) classified as quasars (**class**=‘QSO’). The radial and kinematical distributions of galaxies around the SFCGs covered by the SDSS/MGS are added to the article as additional on-line only material in Figures A2, A3 and A4 of Appendix.

We classify the radial and kinematical distribution of galaxies around each SFCG depending on three number counts:

- n_c number of galaxies inside a circle of 2.5 arcmin centered on the group without any l-o-s velocity constraint. We outline that

this number corresponds just to those group galaxies covered by the Main Galaxy Sample of SDSS, knowing that total number of group galaxies should be larger due to the two situations described below.

- n_v number of galaxies inside a circle of 2.5 arcmin centered on the group and within 1200 km s^{-1} centered at cz_{UV} or the l-o-s velocity of the galaxy nearest to the group center. This corresponds to the number of bound members of the SFCG observed in the SDSS/MGS.
- n_s number of galaxies with a radial projected distance to the group center between 2.5 and 10 arcmin and within 1200 km s^{-1} centered at cz_{UV} or the l-o-s velocity of the galaxy closest to the group center. This number is sampling the richness of a possible galaxy structure where the group is embedded.

An SFCG is considered a real group when it fulfills either of these two conditions:

- $n_v \geq 3$, i.e. at least three velocity-accordant and close galaxy members, or
- $n_c \geq 2$ and $n_v > n_c/2$ i.e. more than half of galaxies observed by the SDSS/MGS being velocity-accordant and close galaxy members. This constraint produces that groups with $n_c=2$ require having $n_v=2$ and groups with $n_c=3$ require having $n_v \geq 2$ to be considered as real groups.

Four situations describing the radial and kinematical distribution of galaxies around each SFCG are considered:

- (a) a real group is considered isolated if $n_s \leq 5$. This is not an extreme constraint of isolation. This constraint only tries to take into account that the UV members could belong to a group also containing other UV faint members and this group could be slightly extended beyond the 2.5 arcmin radius. We are considering that a few galaxies surrounding the SFCG indicate a poor structure.
- (b) a real group is considered to be embedded in a larger galaxy structure (e.g. cluster) if $n_s \geq 6$.

- (c) the SFCG is considered partially the result of a projection effect if, for groups with $n_c \geq 2$ also $n_v \leq n_c/2$ and $n_v \leq 2$.
- (d) the SFCG is framed in the low statistics case and consequently excluded from the previous situations when there is just one or no galaxies in the close neighbourhood of the SFCG i.e. $n_c \leq 1$.

The low statistics case can be the result of two situations. First, the known fiber collision problem in the Main Galaxy Sample of SDSS; two spectroscopic fibers cannot be placed closer than 55 arcsec on a given plate (Strauss et al. 2002). Knowing that the maximum linking length in the FoF algorithm is set to 1.5 arcmin, many of the group galaxies can be closer than the fiber collision distance. In addition, galaxies in SFCGs, which are selected in UV, can be too optically faint and the SDSS/MGS magnitude limit $r' < 17.77$ can reject these galaxies, or they can be relatively bright and have not been observed due to the SDSS/MGS completeness strongly decreasing below $r' \sim 14$ (Montero-Dorta & Prada 2009). Specifically, for the groups identified in a $14.5 \leq r' \leq 18$ SDSS galaxy catalogue by McConnachie et al. (2009), 43 per cent of galaxy members have spectroscopic information available.

For those 139 SFCGs observed by the SDSS/MGS, we obtain the following distribution: 54 SFCGs are isolated groups, 8 SFCGs are embedded in larger galaxy structures, 58 SFCGs are partially the result from a projection effect and 19 SFCGs are considered incompletely covered by the SDSS/MGS. Then, in the case of the group subsample with enough statistics (a)+(b)+(c)=54+8+58=120, we see that a fraction of 52% ((a)+(b)=62 SFCGs) have a significant number of galaxies with accordant l-o-s velocities. We thus expect that roughly half of the entire SFCG sample will be caused by chance projections. It is also found that the fraction of real groups f_{rg} does not present a monotonic trend with n_c (i.e. the number of galaxies with known redshift in the close neighborhood of the group): $f_{\text{rg}}=47 \pm 11\%$ for $n_c=2$, $f_{\text{rg}}=62.5 \pm 8.6\%$ for $n_c=3$ and $f_{\text{rg}}=47.8 \pm 6.0\%$ for $n_c > 3$.

With respect to the close environment of groups, we find a high fraction of isolated groups $54/(54+8)=87\%$. This relatively high fraction

comes from the fact that we are defining here an isolated group as that group which simply is not surrounded by a large galaxy structure such a galaxy cluster but they are clearly distinguishable from its surroundings.

5. Conclusions

This article provides a local sample ($z \lesssim 0.15$) of compact groups of star-forming galaxies. In this type of groups, galaxies strongly interact among themselves and with the rest of the group components (ICM, dark matter halo). This induces morphological changes and star formation events which are currently taking place. The peculiar evolutionary stage of these groups provides a wealth of galaxy observables that may clarify the theoretical framework about galaxy evolution in groups.

We have performed an all-sky search for compact groups of star-forming galaxies in the GALEX UV catalogues. Starting from the 1447 groups initially identified by the Friends-of-Friends group finder, 960 were identified as groups of stellar and/or galactic objects at the outskirts of the two Magellanic Clouds, while another about 200 groups were removed because they did not have, at least 3 UV members compiled as galaxies by NED or, two galaxies within $\Delta z/(1+z)=0.004$. The result from this search are 280 galaxy groups composed by 226, 39, 11 and 4 groups with four, five, six and seven UV members, respectively. Only 59 of the 280 identified SFCGs present a previous catalogued group counterpart in their neighbourhood $D_{\text{sep}} < 2.5$ arcmin. Those groups with a good SDSS spectroscopic coverage show an important fraction of them, roughly half, having a significant number of galaxies with accordant l-o-s velocities. At least, 26 SFCGs are embedded in the infall region of previously catalogued galaxy clusters. A compilation of galaxy redshifts in a sky region of 2.5 arcmin around the SFCG center provides group redshifts for a total of 222 group candidates.

As in all group catalogues, accurate redshifts are required on all galaxy members to remove interlopers or identify blended galaxy objects. In this respect, a full redshift survey of this sample is underway as well as an H α survey of the groups with known redshift. These results may elucidate

several open issues about the evolution of compact groups.

Acknowledgements

The authors would like to thank the referee, Dr. Gary Mamon, for the substantial improvements on the original manuscript that resulted from his recommendations. The article have been improved also thanks to the helpful comments of Christopher P. Haines. J.D.H.F. acknowledges support through the FAPESP grant project 2012/13381-0. C.M.d.O. acknowledges support through FAPESP project 2006/56213-9 and CNPq grant 305205/2010-2. The formal acknowledgements to the resources used in this work can be read at: www.sdss.org/dr6/coverage/credits.html for the Sloan Survey and ned.ipac.caltech.edu for the NED webpage and galex.stsci.edu/GR6/?page=acknowledgments for the GALEX mission. The authors have used the TOPCAT software (Taylor 2005) in this work.

REFERENCES

- Adelman-McCarthy, J. K., Agüeros, M. A., Alam, S. S., et al. 2008, *ApJS*, 175, 297
- Barton, E., Geller, M., Ramella, M., Marzke, R. O., & da Costa, L. N. 1996, *AJ*, 112, 871
- Beers, T. C., Flynn, K., & Gebhardt, K. 1990, *AJ*, 100, 32
- Bianchi, L., Conti, A., & Shiao, B. 2014, *Advances in Space Research*, 53, 900
- Boquien, M., Duc, P.-A., Galliano, F., et al. 2010, *The Astronomical Journal*, 140, 2124
- Cardelli, J. A., Clayton, G. C., & Mathis, J. S. 1989, *ApJ*, 345, 245
- Carroll, S. M., Press, W. H., & Turner, E. L. 1992, *ARA&A*, 30, 499
- Chilingarian, I. V. & Zolotukhin, I. Y. 2012, *MNRAS*, 419, 1727
- Cortese, L., Gavazzi, G., Boselli, A., et al. 2006, *A&A*, 453, 847
- Cox, A. N., ed. 2000, *Allen's Astrophysical Quantities* (Springer-Verlag New York, Inc.)
- Díaz-Giménez, E. & Mamon, G. A. 2010, *MNRAS*, 409, 1227
- Díaz-Giménez, E., Mamon, G. A., Pacheco, M., Mendes de Oliveira, C., & Alonso, M. V. 2012, *MNRAS*, 426, 296
- Domainko, W., Mair, M., Kapferer, W., et al. 2006, *A&A*, 452, 795
- D'Onghia, E., Sommer-Larsen, J., Romeo, A. D., et al. 2005, *ApJ*, 630, L109
- Dressler, A., Oemler, Jr., A., Poggianti, B. M., et al. 2013, *ApJ*, 770, 62
- Duc, P.-A., Brinks, E., Springel, V., et al. 2000, *AJ*, 120, 1238
- Eke, V. R., Baugh, C. M., Cole, S., et al. 2005, *MNRAS*, 362, 1233
- Fujita, Y. 2004, *PASJ*, 56, 29
- Gallagher, S. C., Durrell, P. R., Elmegreen, D. M., et al. 2010, *AJ*, 139, 545
- Gil de Paz, A., Boissier, S., Madore, B. F., et al. 2007, *ApJS*, 173, 185
- Gottlöber, S., Klypin, A., & Kravtsov, A. V. 2001, *ApJ*, 546, 223
- Grebel, E. K. 2007, in *Groups of Galaxies in the Nearby Universe*, ed. I. Saviane, V. D. Ivanov, & J. Borissova, 3–540
- Haines, C. P., Gargiulo, A., & Merluzzi, P. 2008, *MNRAS*, 385, 1201
- Haines, C. P., Pereira, M. J., Sanderson, A. J. R., et al. 2012, *ApJ*, 754, 97
- Hernández-Fernández, J. D., Vílchez, J. M., & Iglesias-Páramo, J. 2012, *ApJ*, 751, 54
- Hickson, P. 1982, *ApJ*, 255, 382
- Hickson, P. 1997, *ARA&A*, 35, 357
- Hickson, P., Mendes de Oliveira, C., Huchra, J. P., & Palumbo, G. G. 1992, *ApJ*, 399, 353
- Hou, A., Parker, L. C., & Harris, W. E. 2014, *MNRAS*, 442, 406
- Huchra, J. P., Macri, L. M., Masters, K. L., et al. 2012, *ApJS*, 199, 26

- Iglesias-Páramo, J. & Vílchez, J. M. 2001, *ApJ*, 550, 204
- Jones, L. R., Ponman, T. J., Horton, A., et al. 2003, *MNRAS*, 343, 627
- Just, D. W., Zaritsky, D., Sand, D. J., Desai, V., & Rudnick, G. 2010, *ApJ*, 711, 192
- Koopmann, R. A. & Kenney, J. D. P. 2004, *ApJ*, 613, 866
- Mahajan, S., Mamon, G. A., & Raychaudhury, S. 2011, *MNRAS*, 416, 2882
- Mamon, G. A. 1986, *ApJ*, 307, 426
- Martin, D. C., Fanson, J., Schiminovich, D., et al. 2005, *ApJ*, 619, L1
- McConnachie, A. W., Patton, D. R., Ellison, S. L., & Simard, L. 2009, *MNRAS*, 395, 255
- McGee, S. L., Balogh, M. L., Bower, R. G., Font, A. S., & McCarthy, I. G. 2009, *MNRAS*, 400, 937
- Mendel, J. T., Ellison, S. L., Simard, L., Patton, D. R., & McConnachie, A. W. 2011, *MNRAS*, 418, 1409
- Mendes de Oliveira, C., Cypriano, E. S., Sodré, Jr., L., & Balkowski, C. 2004, *ApJ*, 605, L17
- Mendes de Oliveira, C., Taylor, K., Quint, B., et al. 2013, *PASP*, 125, 396
- Montero-Dorta, A. D. & Prada, F. 2009, *MNRAS*, 399, 1106
- Morrissey, P., Conrow, T., Barlow, T. A., et al. 2007, *ApJS*, 173, 682
- Moss, C. 2006, *MNRAS*, 373, 167
- Nurmi, P., Heinämäki, P., Sepp, T., et al. 2013, *MNRAS*, 436, 380
- Oman, K. A., Hudson, M. J., & Behroozi, P. S. 2013, *MNRAS*, 431, 2307
- Plana, H., Amram, P., Mendes de Oliveira, C., Balkowski, C., & Boulesteix, J. 2003, *AJ*, 125, 1736
- Ponman, T. J., Allan, D. J., Jones, L. R., et al. 1994, *Nature*, 369, 462
- Prandoni, I., Iovino, A., & MacGillivray, H. T. 1994, *AJ*, 107, 1235
- Proctor, R. N., de Oliveira, C. M., Dupke, R., et al. 2011, *MNRAS*, 418, 2054
- Strauss, M. A., Weinberg, D. H., Lupton, R. H., et al. 2002, *AJ*, 124, 1810
- Taylor, M. B. 2005, in *Astronomical Society of the Pacific Conference Series*, Vol. 347, *Astronomical Data Analysis Software and Systems XIV*, ed. P. Shopbell, M. Britton, & R. Ebert, 29
- Torres-Flores, S., Mendes de Oliveira, C., Amram, P., et al. 2010, *A&A*, 521, A59
- Turner, E. L. & Gott, III, J. R. 1976, *ApJS*, 32, 409
- Urrutia-Viscarra, F., Arnaboldi, M., Mendes de Oliveira, C., et al. 2014, *ArXiv e-prints*
- Verdes-Montenegro, L., Del Olmo, A., Iglesias-Páramo, J. I., et al. 2002, *A&A*, 396, 815
- Walke, D. G. & Mamon, G. A. 1989, *A&A*, 225, 291
- Wetzel, A. R., Tinker, J. L., Conroy, C., & van den Bosch, F. C. 2013, *MNRAS*, 432, 336
- Williams, B. A. & Rood, H. J. 1987, *ApJS*, 63, 265
- Wilman, D. J., Oemler, Jr., A., Mulchaey, J. S., et al. 2009, *ApJ*, 692, 298
- Wyder, T. K., Treyer, M. A., Milliard, B., et al. 2005, *ApJ*, 619, L15
- Zabludoff, A. 2007, in *Groups of Galaxies in the Nearby Universe*, ed. I. Saviane, V. D. Ivanov, & J. Borissova, 249
- Zehavi, I., Zheng, Z., Weinberg, D. H., et al. 2011, *ApJ*, 736, 59
- Zwicky, F., Herzog, E., & Wild, P. 1961, *Catalogue of galaxies and of clusters of galaxies*, Vol. I (California Institute of Technology)
- Zwicky, F., Herzog, E., & Wild, P. 1968, *Catalogue of galaxies and of clusters of galaxies* (California Institute of Technology)

This 2-column preprint was prepared with the AAS L^AT_EX macros v5.2.